Studies on the Breaking Mechanism of Continuous Multifilaments

I. On the stress-strain properties of twisted monofilaments

Bambang MURDIYANTO and Osamu SATO

北海道大学水産学部研究彙報 第29巻 第4号 349-362 頁別刷
昭和53年11月

Reprinted from Bulletin of the Faculty of Fisheries,
Hokkaido University, Vol. 29, No. 4, pp. 349-362

November, 1978

Bull. Fac. Fish. Hokkaido Univ.
29(4), 349-362. 1978.

Studies on the Breaking Mechanism of Continuous Multifilaments

I. On the stress-strain properties of twisted monofilaments

Bambang MURDIYANTO* and Osamu SATO*

Abstract

The problem considered in this study is to arrive at a theoretical calculation for the prediction of the stress-strain curve of twisted monofilament deriving from the known non-twisted monofilament stress-strain curve. It is assumed that a twisted monofilament behaves like a twisted yarn, the fibrils being regarded as fibers or filaments in yarn held together by cohesive forces.

The idea of a neutral zone layer of fibrils where the fibrils length remain unchanged after twisting is here introduced. Two sets of values for the inclination of the angle of fibril (α) in this layer to the monofilament axis, calculated and obtained experimentally, are used in deriving theoretical stress-strain curves. The theoretical stress-strain curves using experimental α give better agreement than the other curves using theoretical α, but a slight discrepancy between theoretical and experimental curves still exsists. This may be supposed in deriving a theoretical calculation, the constancy of Young's modulus during deformation having been adopted, and this may not correspond precisely with the experimental situation. Besides, the inter-fibril frictional forces, if any, were not taken into *account.*

Principal symbols used

	initial	twisted	twisted and strained
Monofilament length	h_0	h_n	h_{nt}
Fibril length	l_0	$l_{n(\theta)}$	$l_{nt(\theta)}$
Monofilament radius	R_0	R_n	R_{nt}
Cylindrical layer radius in inner twisted monofilament	r_0	r_n	r_{nt}
Thickness of cylindrical layer	dr_0	dr_n	dr_{nt}
Radius of neutral zone layer	–	a_n	a_{nt}
Monofilament diameter	d_0	d_n	–

Note: (θ) represents the angle of inclination of fibril to the monofilament axis (twist angle) at any position in the inner zone. (α) represents the twist angle of fibril at the neutral zone layer, and (β) at the monofilament surface.

Introduction

In any study that is concerned with the breaking mechanism of continuous multifilaments, the study on the stress-strain properties of a twisted monofilanent is of importance. The purpose of this study is to make an attempt to determine a basis for the prediction of the stress-strain curve of a twisted monofilament derived

* Laboratory of Fishing Gear Design, Faculty of Fisheries, Hokkaido University.
(北海道大学水産学部漁具設計学講座)

from the known initial (non-twisted) monofilament stress-strain curve. There are some studies of this kind but most of them are in the twisted continuous-filament yarns[1,2,3,4,5]. Concerning the monofilament theory, as in the paper by Zurek, W. et al[6], it is assumed that the twisted monofilament can be considered as twisted yarn, the fibrils being regarded as filaments in yarn held together by cohesive forces.

It might be assumed that, 1) the monofilament has a circular cross section which does not change after the monofilament is twisted, and that the twisted monofilament volume remains constant throughout tensioning, 2) the fibrils of the monofilament possess uniform properties along their length, and all the fibrils are regarded as being identical. The formation of a helicocylindrical structure of the fibril and the disregarding of fibril migration are adopted for the twisted monofilament.

Theoretical aspects

According to the above assumptions, the monofilament may be considered as a long rod with a circular cross section. In this rod we distinguish a cylindrical layer with an inner radius r_0, a thickness dr_0 and a length h_0 (Fig. 1. a). The layers consist of fibrils which are parallel to the rod axis.

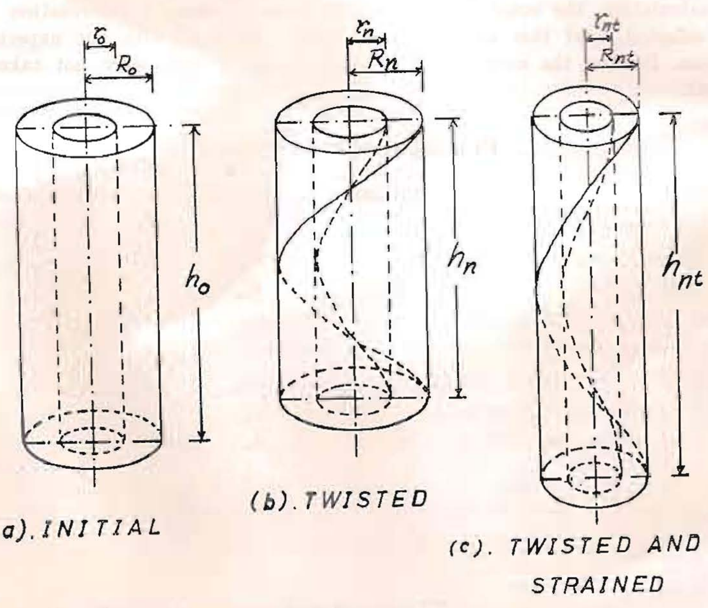

Fig. 1. Geometry of monofilament in initial, twisted, and twisted and strained condition.

After the rod is twisted, its length decreases to h_n and the fibrils at any radius r_0 from the monofilament axis would form a helicocylindrical structure with a helix angle (twist angle) θ to the monofilament axis. Its inner radius becomes r_n and the thickness of the cylindrical layer becomes dr_n (Fig. 1. b). In this case, the radius of any layer r is expressed as a fraction of the monofilament radius R,

$$r = xR\,. \tag{1}$$

So that,
$$dr_0 = R_0 dx\,, \tag{2}$$

$$dr_n = R_n dx\,, \tag{3}$$

$$dr_{nt} = R_{nt} dx\,. \tag{4}$$

In the twisted monofilament the stress in the outer zone results in a compression of the inner zone[6]. There is a neutral zone layer between the outer and inner zones where the fibrils length remain constant. The length of fibrils in this zone is therefore,

$$l_{n(\alpha)} = l_0 = h_0 \operatorname{cec} \alpha\,. \tag{5}$$

The strain of a fibrillar unit in every layer can be calculated as,

$$\varepsilon_n = \frac{l_{n(\theta)} - l_0}{l_0} = \frac{l_{n(\theta)}}{l_{n(\alpha)}} - 1\,. \tag{6}$$

From Fig. 2 it can be seen that

$$\varepsilon_n = \frac{h_n \sec\theta}{h_n \sec\alpha} - 1 = \frac{\sec\theta}{\sec\alpha} - 1\,. \tag{7}$$

The stress in the layer of radius r_n for each fibril is expressed by

$$\sigma_n = E\varepsilon_n = E\left\{\frac{\sec\theta}{\sec\alpha} - 1\right\}, \tag{8}$$

where E is Young's modulus.

The force in the direction of the fibril axis is

$$dW = 2\sigma_n \pi r_n dr_n \cos\theta\,, \tag{9}$$

and its projection upon the monofilament axis becomes

$$dF = dW \cos\theta = 2\sigma_n \pi r_n dr_n \cos^2\theta\,. \tag{10}$$

The sum of these forces must be equal to zero[6]. Assuming that the modulus of compression and that of tension are equal, (this will be plausible in the case of a very small value of the diameter per height of test pieces[7]), then,

$$F = \int dF = \int_0^{R_n} 2\sigma_n \pi r_n dr_n \cos^2\theta\,. \tag{11}$$

The solution of this equation is

$$\sec\alpha_n = \frac{\sec\beta_n - 1}{\ln\sec\beta_n}\,. \tag{12}$$

Let us now observe the geometry of strain for fibrils at the neutral zone layer. After some tensions are given to the twisted monofilament, the fibril will reach the extension ratio $\lambda_{t(\alpha)}$, and the twisted monofilament itself will reach the extension ratio λ_{nt}.

Our fundamental assumption then becomes,

$$\frac{l_{nt(\alpha)}}{l_{n(\alpha)}} = \lambda_{t(\alpha)} = \lambda_t\,, \tag{13}$$

where λ_t is the extension ratio of the non-twisted monofilament. This assumption would appear to be the simplest, which can be made from the mathematical point of view.

According to the assumption of constancy of volume during tensioning, and taking dr_n as the thickness of the neutral zone layer (Fig. 2 and Fig. 3), then

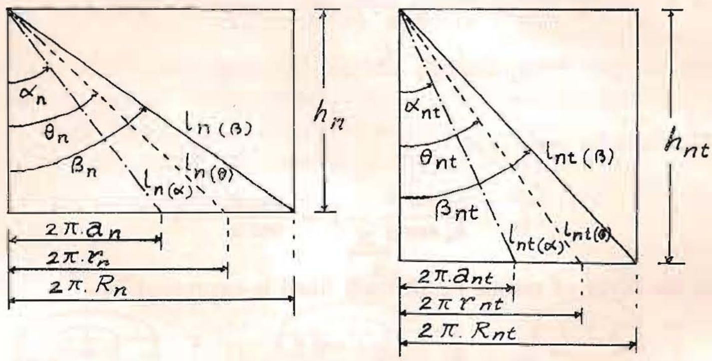

Fig. 2. Opening out of fibril helix from idealized twisted monofilament structure.

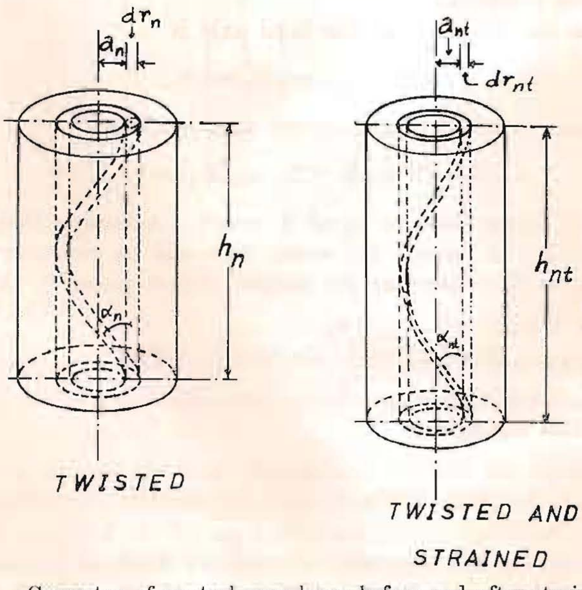

Fig. 3. Geometry of neutral zone layer before and after straining.

$$2\pi a_n dr_n h_n = 2\pi a_{nt} dr_{nt} h_{nt}, \tag{14}$$

$$\pi h_n R_n^2 = \pi h_{nt} R_{nt}^2, \tag{15}$$

and

$$a_{nt} = a_n \lambda_{nt}^{-1/2}. \tag{16}$$

Since the total number of turns does not change during tensioning, the twist angle α_n and α_{nt} (Fig. 2) are related thus:

$$\tan \alpha_{nt} = \lambda_{nt}^{-3/2} \tan \alpha_n. \tag{17}$$

From the Equation 13 and Fig. 2, the relation between λ_t and λ_{nt} can be obtained as

$$\lambda_t^2 \sec^2 \alpha_n = \lambda_{nt}^2 + \lambda_{nt}^{-1} \tan^2 \alpha_n. \tag{18}$$

This is for calculating λ_t at a given λ_{nt} and a twist angle α_n.

Let us now observe the stress in the fibril if some tensional forces F_{nt} are given to the twisted monofilament. The force acting on the direction of the fibril axis being

$$\begin{aligned} dW &= 2\sigma_n \pi r_{nt} dr_{nt} \cos \theta_{nt} \\ &= 2E \varepsilon_{nt} \pi r_{nt} dr_{nt} \cos \theta_{nt}. \end{aligned} \tag{19}$$

The projection of this force upon the monofilament axis becomes

$$dF_{nt} = dW \cos \theta_{nt} = 2E \cdot \varepsilon_{nt} \pi r_{nt} dr_{nt} \cos^2 \theta_{nt}. \tag{20}$$

If $\varepsilon_{nt(\alpha)}$ was the strain of the fibril at the neutral zone layer, then we can calculate that

$$dF_{nt} = 2E\pi \left\{ \frac{\sec \theta_{nt}}{\sec \alpha_{nt}} (\varepsilon_{nt(\alpha)} + 1) - 1 \right\} \cos^2 \theta_{nt} r_{nt} dr_{nt}, \tag{21}$$

and

$$F_{nt} = \int_0^{R_{nt}} dF_{nt} = E \varepsilon_{nt(\alpha)} \frac{h_{nt}^2}{4\pi} \ln \sec^2 \beta_{nt}. \tag{22}$$

The stress in the strained twisted monofilament is calculated as the nominal stress, i.e.

$$\sigma = \frac{F_{nt}}{\pi R_n^2}, \tag{23}$$

and this is equal to

$$\frac{F_{nt}}{\pi R_n^2} = \frac{E \varepsilon_{nt(\alpha)} h_{nt}^2 \ln \sec^2 \beta_{nt}}{4\pi^2 R_n^2}. \tag{24}$$

Remembering the constancy of volume during tensioning, we can obtain

$$\tan \beta_{nt} = \lambda_{nt}^{-3/2} \tan \beta_n, \tag{25}$$

and Equation 24 becomes

$$\frac{F_{nt}}{\pi R_n^2} = E\,\varepsilon_{nt(\alpha)}\,\frac{\lambda_{nt}^2 \ln(1+\lambda_{nt}^{-3}\tan^2\beta_n)}{\tan^2\beta_n}\,. \tag{26}$$

Now we can simply write Equation 26 as

$$\sigma = \sigma_{nt(\alpha)} C\,, \tag{27}$$

where,

σ = the stress in the twisted monofilament,

$\sigma_{nt(\alpha)}$ = the stress in the fibril at the neutral zone layer,

$$C = \frac{\lambda_{nt}^2 \ln(1+\lambda_{nt}^{-3}\tan^2\beta_n)}{\tan^2\beta_n}\,.$$

Now we can derive theoretical stress-strain curves of a twisted monofilament from the non-twisted monofilament curve using Equation 18 to calculate the strain and Equation 27 for the calculation of the corresponding stress.

The procedure for the calculation of the stress-strain curve is first to compute, the value of λ_t (using Equation 18) for the fibril at the neutral zone layer or for the non-twisted monofilament, from a given value of the twist angle α and a series of λ_{nt} from 1.01 up to the maximum required (at about 80% of the monofilament breaking strength) at interval 0.01. The corresponding stress ($\sigma_{nt(\alpha)}$) is then obtained from the initial curve. These data are then inserted into Equation 27 together with the relevant values of λ_{nt} before plotting into the graph. These operations are repeated for various degrees of the twist angle α (theoretical and experimental values) and β as it is required. The results of the above calculations are then compared with the experimental curves.

Materials and methods

Nylon monofilaments of various thickness were used as experimental materials (Table 1). To determine the changes of length and diameter, a monofilament about 1 m in length was vertically hung and twisted. The upper end of the monofilament was fixed in a chuck and during the twisting the lower end was loaded with a weight as its initial tension and to prevent snarling. A mark on the monofilament was observed by the use of a travelling microscope to determine the

Table 1. *Nylon monofilaments used for experiments*

No.	Initial diameter (mm)	Young's modulus* (kg/mm^2)
4	0.324	306
16	0.659	426
18	0.705	426
40	1.068	420
60	1.316	280
80	1.527	520

*) measured at the beginning of the stress-strain curve.

change of length. The diameter change was measured by using a micrometer. Ten tests were carried out for each experiment to obtain the mean value. These experiments were carried out at room temperature ranging from 17°–25°C and relative humidity varying from 50% to 70%, on dry condition.

The twist angle β was obtained from

$$\beta = \tan^{-1} \frac{\pi d_n N}{h_n}, \tag{28}$$

where N=number of twists.

To obtain the stress-strain curve, from the load elongation curve, experiments were carried out using a Strength Testing Machine (Shimadzu Autograph S–2000) and an Extensometer (Shimadzu Extensometer SE–5) as a combination apparatus (Fig. 4). The schematic diagram of the experimental apparatus is shown in Fig. 5. The experiments were carried out as follows. A nylon monofilament test

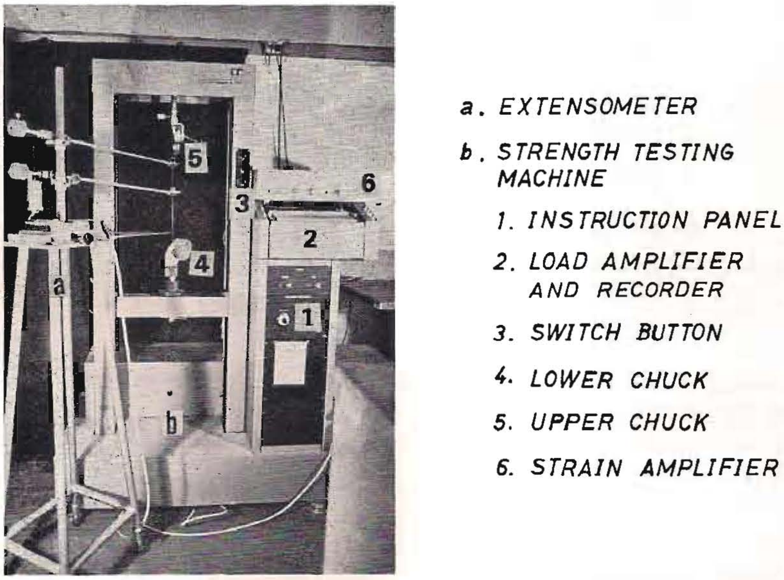

Fig. 4. Apparatus for measuring load elongation curve.

piece of 1 m in length was fixed in the upper chuck of the strength tester. Then a certain number of twists was given using a simple hand drill at the lower end before it was fixed in the lower chuck. A certain length of 100 mm of this test piece was fixed by stoppers (chucks to determine the initial length for the measurement of strain) of the extensometer. By operating the strength tester, the monofilament was stretched until about 80% of its breaking point and the load elongation curve was recorded in the recorder. Measurements were repeated 10 times with each sample. The tensile speed was 300 mm/min at room temperature of 17°–25°C and humidity 60–75%.

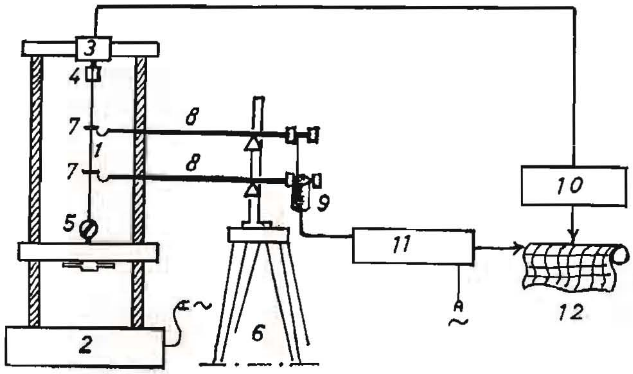

1. TEST PIECE
2. STRENGTH TESTING MACHINE
3. LOAD CELL
4. UPPER CHUCK
5. LOWER CHUCK
6. EXTENSOMETER
7. STOPPER
8. EXTENSOMETER ARM
9. DIFFERENTIAL TRANSFORMER
10. LOAD AMPLIFIER
11. STRAIN AMPLIFIER
12. GRAPH RECORDER

Fig. 5. Schematic diagram of apparatus for measuring load elongation curve.

Result and Discussion

The change in length of the monofilament by twist is shown in Fig. 6. Fig. 7 is showing the change in diameter of the monofilament by twist. The formulation of experimental data into experimental formula results like this:

$$\frac{h_n}{h_0} = e^{\left(\frac{-3.91}{10^6}\beta^{2.79}\right)}, \tag{29}$$

for the change in length by twist, and

$$\frac{d_n}{d_0} = e^{\left(\frac{2.64}{10^5}\beta^{2.11}\right)}, \tag{30}$$

for the change in diameter of the monofilament by twist.

The stress-strain curves of monofilaments, initial and twisted conditions, were obtained from load elongation relationships by putting the nominal stress instead of load in the ordinate, i.e. the corresponding load per unstrained cross sectional area. The abscissa shows the monofilament strain. Fig. 8 up to Fig. 10 are examples of experimental stress-strain curves obtained in this way.

Fig. 11 up to Fig. 13 show the comparison between the experimental and two sets of calculated stress-strain curves. One set was calculated using α from

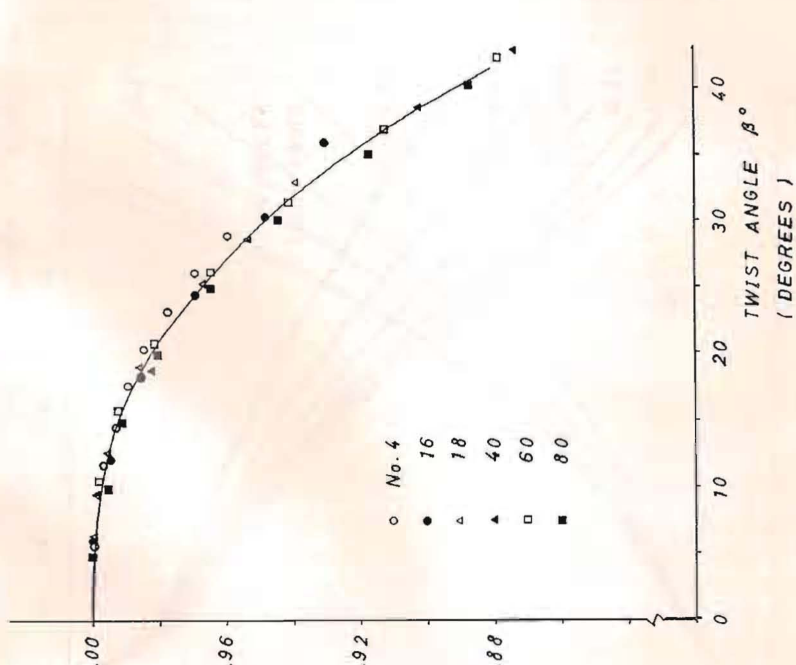

Fig. 6. Change in length of monofilament by twist at various twist angles.

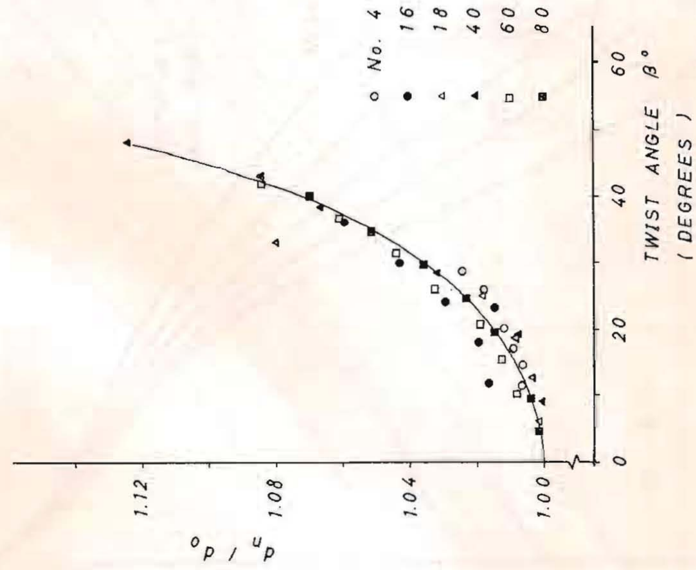

Fig. 7. Change in diameter of monofilament by twist at various twist angles.

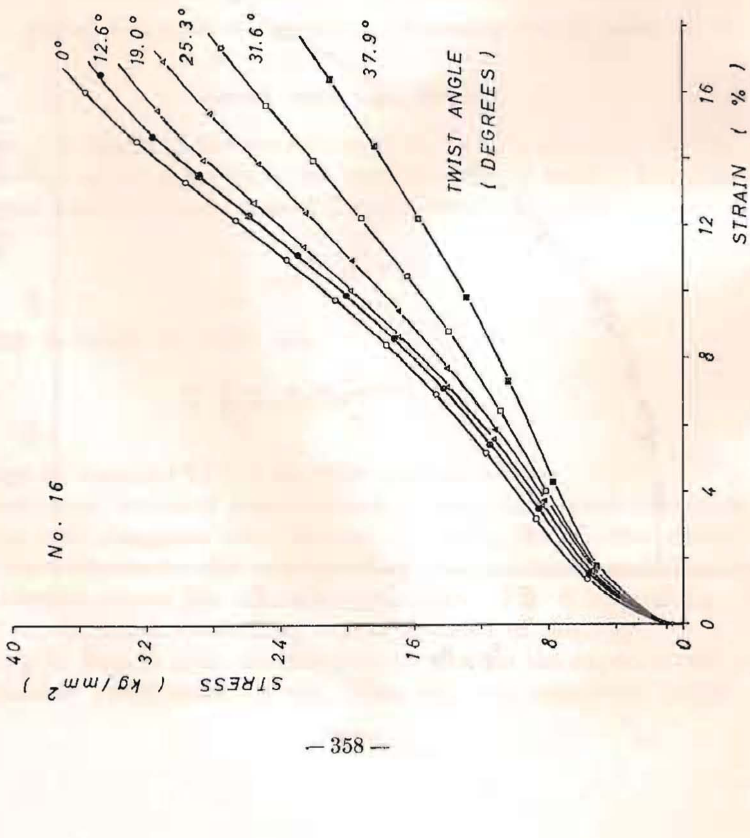

Fig. 8. Experimental stress-strain curves of nylon monofilament No. 16 at various twist angles.

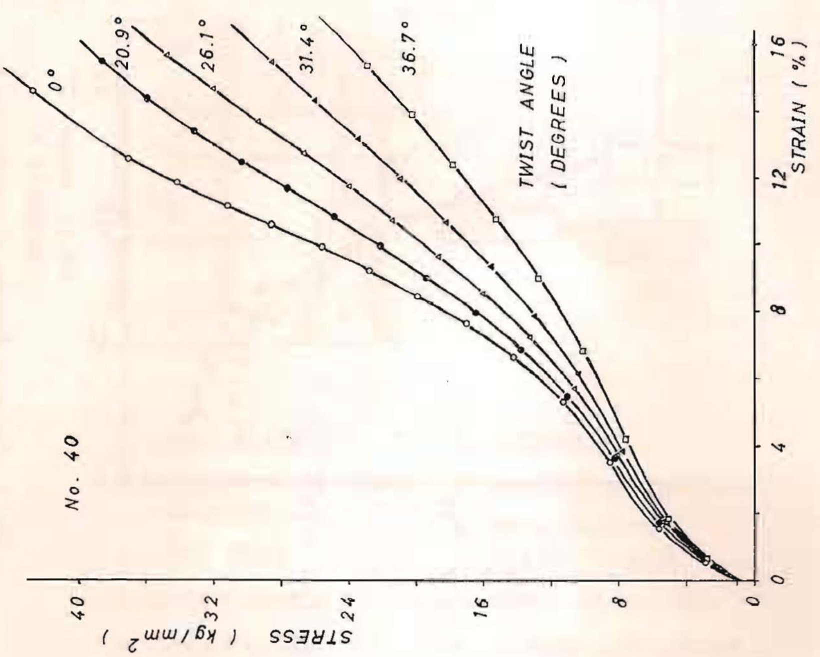

Fig. 9. Experimental stress-strain curves of nylon monofilament No. 40 at various twist angles.

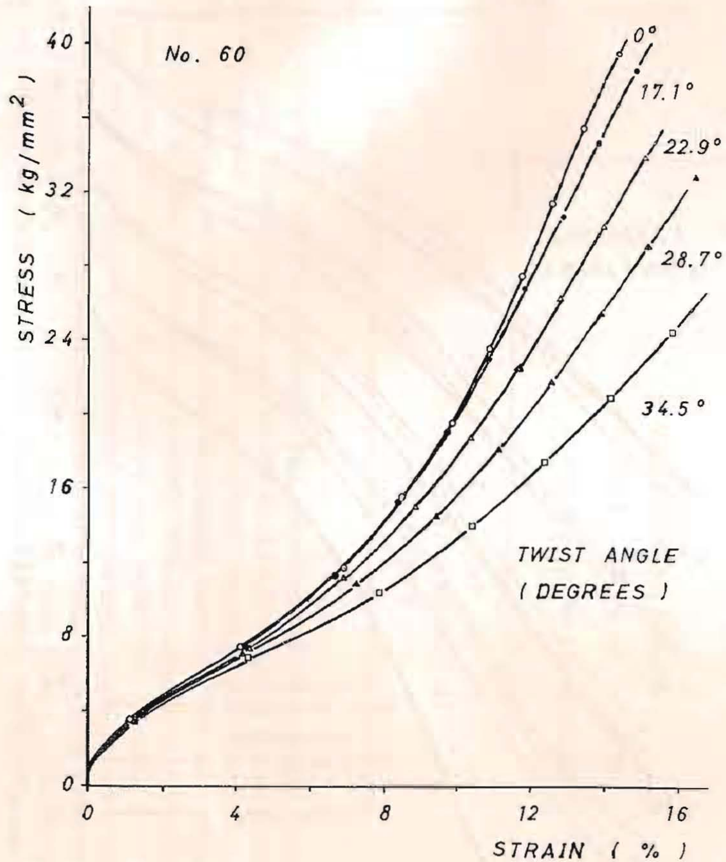

Fig. 10. Experimental stress-strain curves of nylon monofilament No. 60 at various twist angles.

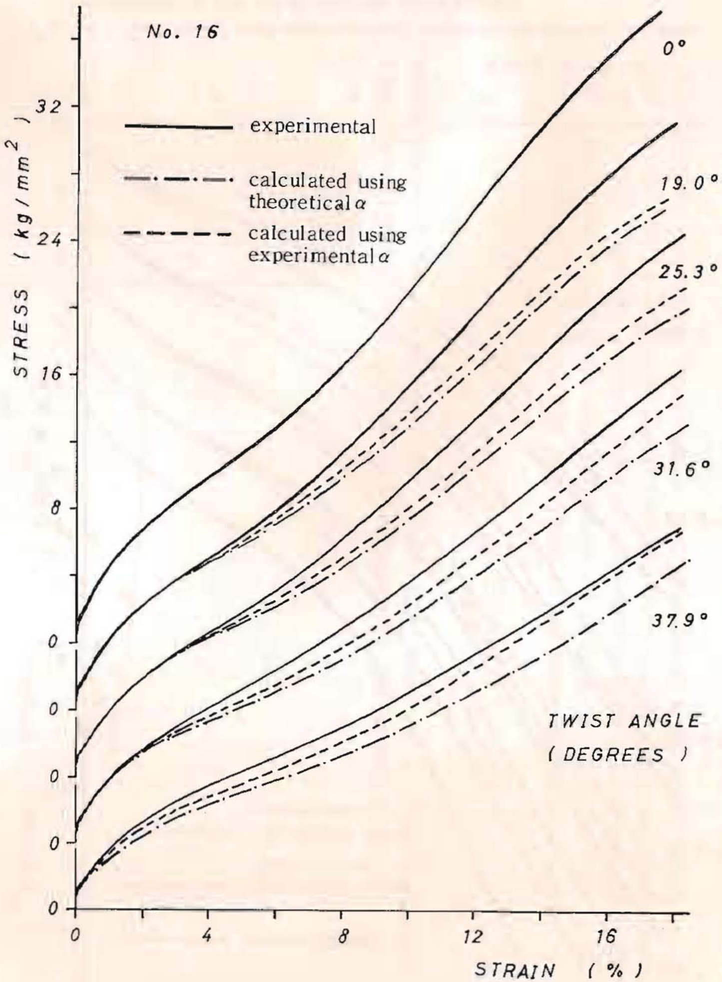

Fig. 11. Calculated and experimental stress-strain curves of nylon monofilament No. 16 at various twist angles.

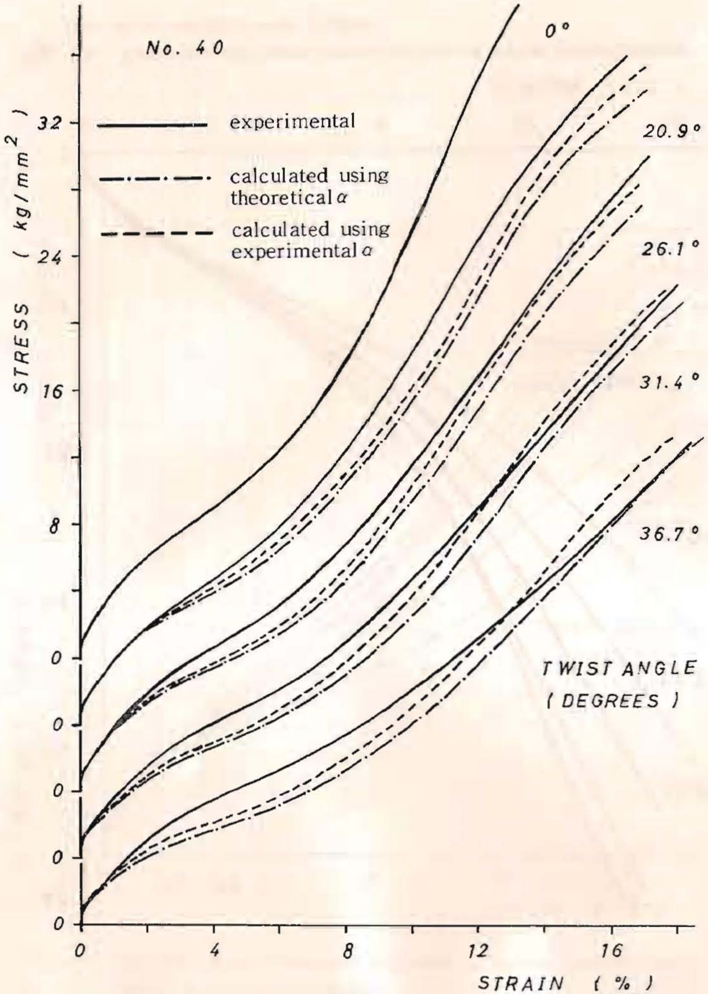

Fig. 12. Calculated and experimental stress-strain curves of nylon monofilament No. 40 at various twist angles.

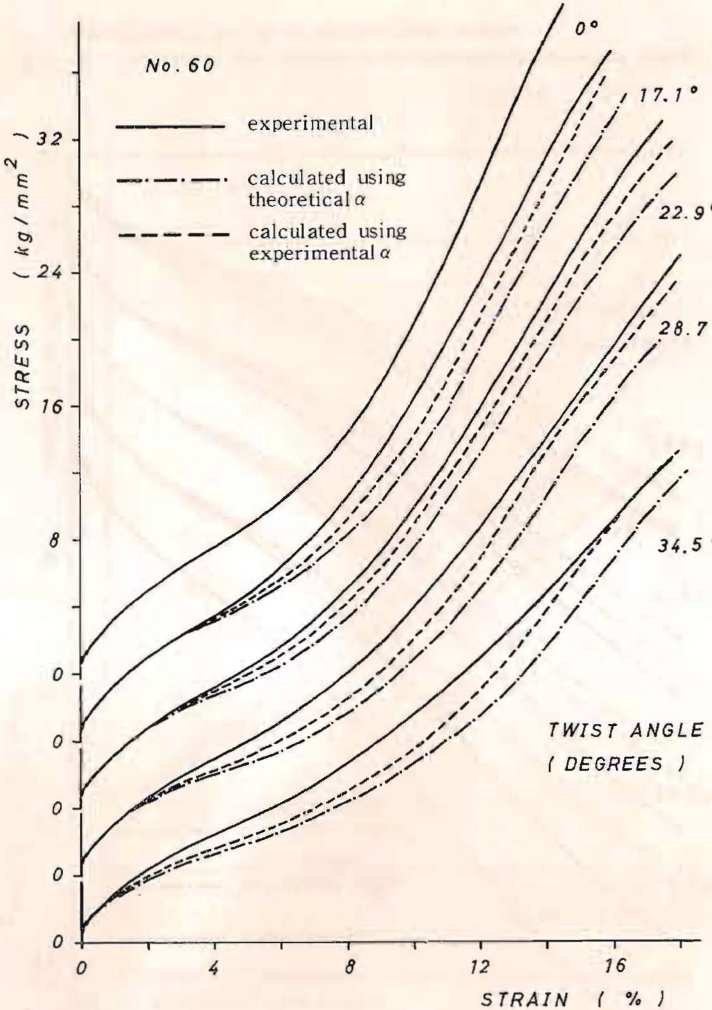

Fig. 13. Calculated and experimental stress-strain curves of nylon monofilament No. 60 at various twist angles.

experimental values and the other set was calculated using α derived from Equation 12. It can be seen that the theoretical curve using the experimental value of α gives better agreement than using the theoretical α to the experimental curves. This phenomenon is due to the differences of both α values. In Fig. 14 can be seen the differences between the two kinds of α values represented as

$$k=\frac{a_n}{R_n}=\frac{\tan\alpha}{\tan\beta}\,. \tag{31}$$

where the solid line represents the theoretical value of k, drawn against the experimental value of k for various thicknesses of the monofilament.

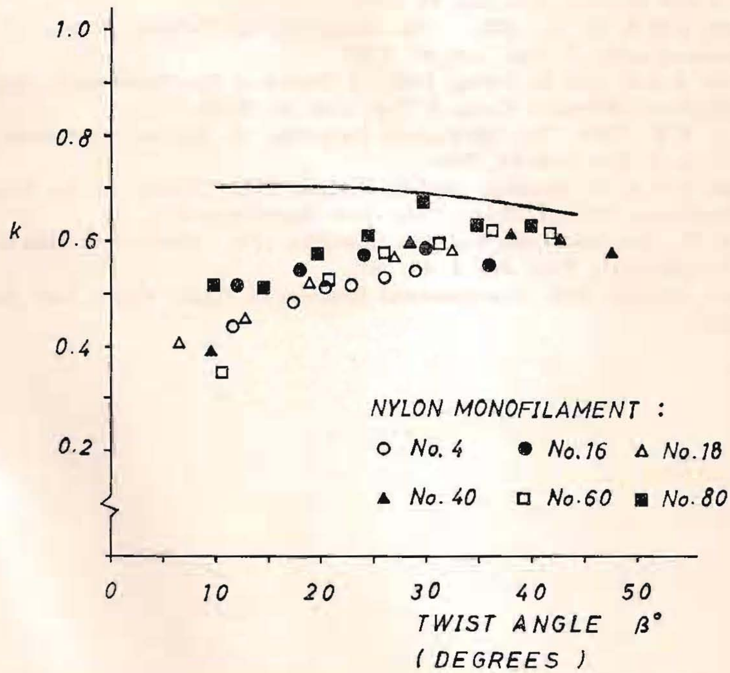

Fig. 14. Radius of neutral zone layer represented by k at various twist angles.

Some deviations between calculated and experimental stress-strain curves have been found. These deviations may be due to the following; 1) the modulus of elasticity is regarded to be constant throughout twisting and tensioning in deriving the theoretical calculation for the stress-strain curve and the neutral zone layer position. This may not correspond precisely with the experimental situation, 2) the assumption that the fibrils at the neutral zone layer have the same form of stress-strain curve with that of a non-twisted monofilament might be a weakness in the theoretical point of view since the fibrils bear to some degrees of twisting in the twisted monofilament, but it is difficult to see on what basis a more realistic assumption could be arrived at, and 3) the theory in this study has been developed without any notice on the interfibril frictional forces and how it varies during deformation.

Acknowledgements

The authors wish to acknowledge their sincere gratitude to Dr. K. Nashimoto and Mr. K. Yamamoto of this Faculty for their suggestions and for reviewing the manuscript.

References

1) Hearle, J.W.S., H.M.A.E. El Behery and V.M. Thakur. 1960. The Mechanics of Twisted Yarns. *J. Text. Inst.* **51**, T299.
2) Hearle, J.W.S. et al. 1961. The Mechanics of Twisted Yarns: Theoretical Developments. *J. Text. Inst.* **52**, T191.
3) Treloar, L.R.G., and G. Riding. 1963. A Theory of The Stress-strain Properties of Continuous-Filament Yarns. *J. Text. Inst.* **54**, T156.
4) Kilby, W.F. 1964. The Mechanical Properties of Twisted Continuous-Filament Yarns. *J. Text. Inst.* **55**, T591.
5) Hearle, J.W.S., P. Grosberg, and S. Backer. 1969. Theory of the Extension of Continuous Filament Yarn. *New York Interscience.* 175.
6) Zurek, W., Romualda Cislo, and Ewa Kowalska. 1976. Elastic Properties of Twisted Monofilaments. *Text. Res. J.* **46**, 381.
7) Backer, Stanley. 1960. Compressional Behavior of Textile Fibers. *Text. Res. J.* **30**, 405.